Original Articles

Extended patchy ecosystems may increase their total biomass through self-replication

Mustapha Tlidi[a,*], Ignacio Bordeu[b], Marcel G. Clerc[c], Daniel Escaff[d]

[a] Département de Physiquen Faculté des Sciences, Université Libre de Bruxelles (ULB), Campus Plaine, CP. 231, B-1050 Bruxelles, Belgium
[b] Department of Mathematics and Centre for Doctoral Training on Theory and Simulation of Materials, Imperial College London, 180 Queen's Gate, London SW7 2AZ, United Kingdom
[c] Departamento de Física, Facultad de Ciencias Físicas y Matemáticas, Universidad de Chile, Casilla 487-3, Santiago, Chile
[d] Complex Systems Group, Facultad de Ingeniería y Ciencias Aplicadas, Universidad de los Andes, Monseñor Alvaro del Portillo 12.455, Las Condes, Santiago, Chile

A R T I C L E   I N F O

A B S T R A C T

Patches of vegetation consist of dense clusters of shrubs, grass, or trees, often found to be circular characteristic size, defined by the properties of the vegetation and terrain. Therefore, vegetation patches can be interpreted as localized structures. Previous findings have shown that such localized structures can self-replicate in a binary fashion, where a single vegetation patch elongates and divides into two new patches, in a process resembling cellular mitosis. Here, we extend these previous results by considering the more general case, where the plants interact non-locally, this extension adds an extra level of complexity and shrinks the gap between the model and real ecosystems, where it is known that the plant-to-plant competition through roots and above-ground facilitating interactions have non-local effects, i.e. they extend further away than the nearest neighbor distance. Through numerical simulations, we show that for a moderate level of aridity, a transition from a single patch to periodic pattern occurs. Moreover, for large values of the hydric stress, we predict an opposing route to the formation of periodic patterns, where a homogeneous cover of vegetation may decay to spot-like patterns. The evolution of the biomass of vegetation patches can be used as an indicator of the state of an ecosystem, allowing to distinguish if a system is in a self-replicating or decaying dynamics. In an attempt to relate the theoretical predictions to real ecosystems, we analyze landscapes in Zambia and Mozambique, where vegetation forms patches of tens of meters in diameter. We show that the properties of the patches together with their spatial distributions are consistent with the self-organization hypothesis. We argue that the characteristics of the observed landscapes may be a consequence of patch self-replication, however, detailed field and temporal data is fundamental to assess the real state of the ecosystems.

1. Introduction

Spontaneous shift from a uniform cover of vegetation into a fragmented ecosystem constituted by a spatially periodic distribution of gaps, or patches, is a well documented issue in plant ecology. This transition may occur either in water or nutrient limited territories. It is now widely admitted that facilitative and competitive interactions between individual plants can directly or indirectly account for the formation of vegetation patterns (Lefever and Lejeune, 1997; Klausmeier, 1999; HilleRisLambers et al., 2001; von Hardenberg et al., 2001; Tlidi et al., 2008; Vesipa et al., 2015). The spatial distribution of such patterns can be modified by the effect of climatic, terrain and anthropogenic influences (Kefi et al., 2007; Kefi et al., 2007; Dakos et al., 2011; Deblauwe et al., 2012). Quantitative studies based on field

observations have been made on: the Sahelian gapped patterns, constituted by Combretum micranthum trees (Barbier et al., 2006; Barbier et al., 2008; Lefever et al., 2009); patches of vegetation in arid high altitude environments in the tropical alpine ecosystems of the Andes formed by Festuca orthophylla (Poaceae); and for grasses or by Pycnophyllum tetrastichum cushions (Bolivia, Couteron et al., 2014).

Patterned vegetation landscapes are fragmented, i.e, the terrain is only partially covered by vegetation. Some of these landscapes are composed of vegetation patches, which may be sparsely or regularly distributed. These patches usually have a characteristic size and well defined circular shape. It has been shown recently that localized patches can be destabilized by a deformation of their circular shape, either leading to the formation of labyrinthine patterns (Bordeu, 2016), or dividing into two new identical patches of smaller diameter (Bordeu

---

* Corresponding author.
E-mail addresses: mtlidi@ulb.ac.be (M. Tlidi), ibordeu@imperial.ac.uk (I. Bordeu).

et al., 2016). The latter is a phenomenon often called self-replication and resembles mitotic cell division. It has been studied in the context of herbaceous populations in arid ecosystems (Bordeu et al., 2016). The self-replication mechanism allows the transition from a single localized structure into a qualitatively different state, namely a hexagonal periodic pattern of vegetation. During the transition from localized to periodic pattern, the total biomass increases as newly formed patches contribute to the repopulation of the territory accessible to vegetation. From a theoretical point of view, self-replication is a patterning phenomenon better known in physico-chemical contexts rather than ecological systems. It is a generic mechanism of pattern formation, which has been observed and established in various non-equilibrium systems, such as chemical systems (Pearson, 1993; Lee et al., 1994; Kaminaga et al., 2005; Kolokolnikov and Tlidi, 2007), in plant ecology (Meron et al., 2004; Bordeu et al., 2016, and nonlinear optics Tlidi et al., 2002).

In this contribution, we investigate the space-time dynamics of vegetation under a self-replication phenomenon by extending the previous work by Bordeu et al. (2016), Bordeu (2016), where a simple local model was used to illustrate that self-replication was a possible mechanism for vegetation propagation. Here we consider a general integro-differential model instead of the simplified model of Bordeu et al. (2016), Bordeu (2016), where non-local interactions are taken explicitly into account. The non-localities arise from the facilitating mechanisms, i.e. promoters of vegetation growth, competition mechanisms, which limit vegetation growth, and dispersion effects. This model corresponds to a variant of the theory of vegetation patterning established by Lefever and Lejeune (1997), which focuses on the relationship between the structure of individual plants and the facilitation-competition interactions existing within plant communities. It is now widely recognized that the existence of facilitation and competition interactions play an important role in the formation of self-organized vegetation patterns. Numerical simulations of our model show indeed a self-replication process that leads moderately arid ecosystems to undergo a transition to higher biomass states, namely hexagonal patterns of vegetation patches. Moreover, we show that this kind of patterns may be obtained through the decay of a homogeneous vegetated landscape towards a less populated fragmented state, where hydric stress induces contraction of vegetated areas. Depending on the levels of aridity, the ecosystems may decay to a different type of patterned states or even become desert.

We study the characteristics of both self-replication and fragmentation processes through the analytic and numerical analysis of a general integro-differential model. We show, from a theoretical perspective, that depending on the levels of aridity localized patches can be more or less stable than the periodic pattern, a phenomenon previously studied in simpler local models (Vladimirov et al., 2011). In an attempt to conciliate the theoretical observations with real data, we consider two ecosystems, namely, from Zambia and Mozambique, these landscapes are composed of vegetation patches reaching large sizes, of the order of tens of meters in diameter (see Fig. 1). We perform statistical analysis of satellite images and find that patches have correlated characteristic patch sizes and inter-patch distances along with other properties that support the hypothesis of the self-organization nature of these landscapes.

The article is organized as follows: in Section 2.1 the theoretical model is introduced, together with the phase diagram. A description of the methods used to analyze the satellite images are included in Section 2.3. The results are presented in Section 3. Theoretical results indicating the relationship with the wavelength and the range of the facilitative and competitive interactions are presented in the appendix. Finally, we present the Discussion, Conclusions and Perspectives of our work.

2. Methods

2.1. Mathematical model

The modeling of ecosystems is a challenging and complex problem. Here, we adopt the theory of vegetation patterns established by R. Lefever and coworkers two-decades ago to model the spatiotemporal dynamics of vegetation in which both space and in time are considered to be continuous variables (Lefever and Lejeune, 1997). This theory incorporates the non-local facilitative and the competitive plant-to-plant interactions though kernels (Lefever and Lejeune, 1997; Tlidi et al., 2008; Lefever et al., 2009; Lefever and Turner, 2012). In the absence of these interactions, the resulting model is similar to the paradigmatic logistic equation introduced by Verhulst to study population dynamics (Verhulst, 2013; Mawhin, 2002). In what follows we consider vegetation of a single species settled on a flat landscape under isotropic and homogeneous environmental conditions. To simplify further the description of the system, we assume that all plants are mature. Thus, we neglect age classes. This approximation can be justified by the fact that individual plants grow on much faster time scale comparing to the time scale of the formation of regular vegetation pattern. The only variable is the vegetation biomass density which is defined at the plant level. Let us introduce the biomass density, $b(\mathbf{r},t)$, that satisfies the following dynamical evolution (Tlidi et al., 2008; Lefever et al., 2009)

$$\partial_t b(\mathbf{r},t) = b(\mathbf{r},t)[1-b(\mathbf{r},t)]M_f(\mathbf{r},t) - \mu b(\mathbf{r},t)M_c(\mathbf{r},t) + DM_d(\mathbf{r},t), \quad (1)$$

where $\mathbf{r}$ and t are the spatial coordinates and time, respectively. The time derivative is represented by ∂_t. The parameter μ, is the decay-to-growth rate ratio. It can be viewed as an indirect measure of resource scarcity or stress, that limits net biomass production and is what we refer to as aridity parameter. The first and the second terms on the right-hand-side of Eq. (1) account for the plant-to-plant facilitation and competition feedbacks, respectively. They describe the spatial extension of feedback effects in terms of the characteristic ranges L_f and L_c over which facilitative and competitive interactions operate, respectively. The facilitative interaction acts on the level of the aerial plant structure (crown) that involves sheltering, litter, water funneling or any other effect, such as seed production and germination that contribute to the
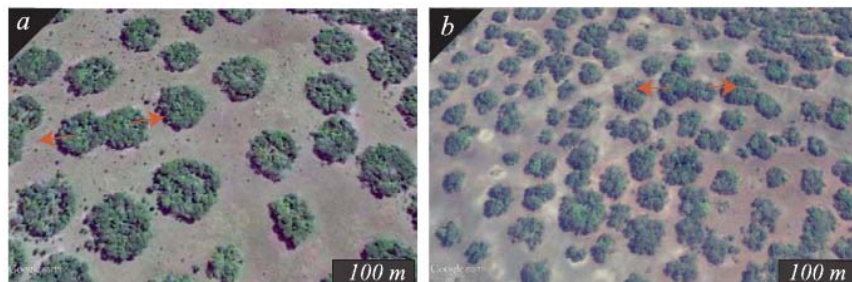

Fig. 1. Satellite images (*Google Earth Pro*), of vegetation patches in (a) the Mufumbwe District in the North-Western Province of Zambia [13°46′39.83″S, 25°16′39.59″E], and (b) the Fombeni, Mozambique [18°41′02.17″S, 35°31′55.95″E]. The red arrows indicate overlapping patches, possibly undergoing self-replications.

biomass natural growth (Brooker et al., 2008). Let L_a be the crown radius projected on the surface element $A = \pi L_a$ centered on a point $\mathbf{r}$. Assuming that the length of facilitative interaction is equals to the radius of the crown, i.e., $L_f = L_a$. On the other hand, in resource-limited environments, plants should compete for their survival. In face of climate change and increasing drought periods, plants should adapt their root structures to overcome resource scarcity (Schenk and Jackson, 2002; Barbier et al., 2006). Through their root structures (rhizosphere), each individual plant tends to deprive its neighbors of vital resources, such as water or nutrient uptake. Measurements of roots lateral spread indicate that they extend beyond the radius of the aerial structure (crown) by an order of magnitude (Barbier et al., 2006; Barbier et al., 2008; Lefever et al., 2009; Couteron et al., 2014).

The competitive interaction between plants tends to oppose the facilitation mechanisms, by impeding vegetation growth. In arid landscapes, the length of facilitative interaction (crown) is much shorter than the length of the competitive interaction operating at the level of the rhizosphere which is the volume of soil around living roots. Let consider also that the range of the competition is such that $L_c = L_r$, where, L_r is the radius of the rhizosphere. The third term in Eq. (1) describes the spatial propagation of vegetation via seed dispersal. The parameter D is the rate of propagation of the vegetation. The competitive plant-to-plan interaction is considered to be of the form

$$M_c(\mathbf{r},t) = \exp\left(\frac{\chi_c}{N_c} \int e^{-|\mathbf{r}'|/L_c} b(|\mathbf{r} + \mathbf{r}'|,t) d\mathbf{r}'\right), \tag{2}$$

where, χ_c is the strength of the competitive interaction, and N_c is a normalization constant, that depends on the spatial dimension. In two dimensions, $N_c = 2\pi L_c^2$. The spatial propagation of vegetation via seed dispersion is assumed to have the form

$$M_d(\mathbf{r},t) = \frac{\delta}{\pi} \int e^{-|\mathbf{r}'|^2/L_d^2} [b(\mathbf{r} + \mathbf{r}',t) - b(\mathbf{r} t)] d\mathbf{r}', \tag{3}$$

the parameter L_d and δ are, respectively, the dispersion range of seeds and the strength of dispersive process. To simplify further the analysis we assume that the seed dispersion is described as diffusion $M_d(\mathbf{r},t) \approx D\nabla^2 b(\mathbf{r},t)$. This can be obtained by considering a small dispersion range and a simple Taylor expansion, which leads to $D = \delta L_d^4/4$. To simplify further the problem, we consider that the facilitation is well described by a local process modelled by $M_f(\mathbf{r},t) = \exp(\chi_f b)$, where χ_f is the strength of the facilitative interaction.

The analysis we make in this work generalizes previous results. Here, the complete non-local integro-differential model is analyzed, which accounts for an important step forward in the understanding of the behavior of this type of system. For a complete linear stability analysis of this model see Appendix A.1.

2.2. Localized vegetation patches

The non-local Eq. (1) exhibits stable circular localized structures which are supported by one of the homogeneous steady state, $b_0 = 0$ (unpopulated state) or b_s (homogeneously vegetated). In the context of vegetation dynamics, localized structures that emerge from the unpopulated state $b_0 = 0$, correspond to circular patches of vegetation which are surrounded by bare terrain. As previously mentioned, periodic states and localized patches emerge as a self-organizing response of the system to changes in the parameters. Aridity (μ), is of particular interest, as it can be directly related to field measurements, and also relates to an ever-increasing concern due to global warming. An increase in aridity (lower hydric resources available or other stress factors) may cause a contraction of savannas and woodlands, in a process called desertification, triggering the formation of vegetation patterns or even deserts. The necessary and sufficient condition for the formation of localized patches is the coexistence between a homogeneous cover and a periodic vegetation pattern. Implying the existence of an hysteresis loop. Inside this loop, there is a so-called pinning range of the aridity

parameter where localized gaps or patches are stable (Lejeune et al., 2002; Rietkerk et al., 2004; Tlidi et al., 2008). Similar pinning behavior occurs in many spatially extended systems where a homogeneous steady state coexists with a spatially periodic state (Pomeau, 1986; Tlidi et al., 1994; Champneys, 1998; Coullet et al., 2000). Pinning was first reported for front solutions by Pomeau (1986), and has also been applied to gap vegetation patterns (Vladimirov et al., 2011). Localized structures and localized patterns are a well documented phenomenon, concerning almost all fields of natural science including chemistry, biology, ecology, physics, fluid mechanics, and optics (Tlidi et al., 2014; Knobloch, 2015; Meron, 2015).

In addition to analytically deriving predictions from Eq. (1), we will provide a case study for which the interpretation of vegetation patchiness based on localized structures and self-replication is plausible.

2.3. Data analysis

Through the use of satellite images obtained from *Google Earth*, we have located regions in Zambia and Mozambique where vegetation patches dominate the landscape (see Supplementary information, Table 1).

2.4. Patch detection algorithm

In order to detect the vegetation, we developed a simple algorithm that segments the images, detects vegetation patches and extract properties of interest (Matlab vR2016b, see Supplementary Information 6.1). The boundaries of every detected patch are used to extract the patch geometrical features, such as area, perimeter, equivalent diameter, and centroid positions, which are then used in the spatial analysis.

2.5. Equivalent radius and nearest-neighbor distance

The equivalent radius of each structure r_{eq} is calculated as

$$r_{eq} = \sqrt{\frac{A_s}{\pi}} \tag{4}$$

where A_s corresponds to the area of the structure. The nearest neighbor distances is obtained by finding the minimum of the distance every patch and all the other patches.

2.6. Spatial distribution analysis

2.6.1. L-function

For the analysis of the spatial distribution of patches we make use of the modified Ripley's function L, for this, only the centroids of the patches are used. We define L as (Ripley, 1976)

$$L(r) = \sqrt{\frac{A}{\pi N^2} S(r)} \tag{5}$$

where r is the distance from the reference point. N and A are the total number of points and the area, respectively. $S(r)$ is the number of points that lay inside a circle of radius r centered on a patch of reference chosen randomly, this is repeated for multiple patches. As control we compute the L function for a set of randomly distributed point (null model), by repeating this 200 times, construct the 95% confidence intervals. When the observed values of L go above (below) the confidence interval, we say the distribution of point is clustered (dispersed).

2.6.2. Radial distribution function

Similarly to the L-function, the radial distribution function $g(r)$, is computed using only the positions of the centroids of the detected objects, we define $g(r)$ as (Couteron and Kokou, 1997)

$$g(r) = \frac{N(r)}{2\pi r \Delta r \rho} \qquad (6)$$

where $N(r)$ is the number of points that lie inside a ring of radius r and width Δr, centered on a given object. The numerator of this expression corresponds to the total number of points that lay inside the ring for the case of homogeneously distributed objects, ρ is the overall number density. The radial distribution function, $g(r)$, measures the correlation of the position of the points, values of $g(r) > 1$ ($g(r) < 1$) indicate positive (negative) correlation. N(r) in numerically computed by measuring the distance between every two patches in the images, and then performing a histogram, where the bin-width corresponds to Δr.

2.6.3. Fourier transform

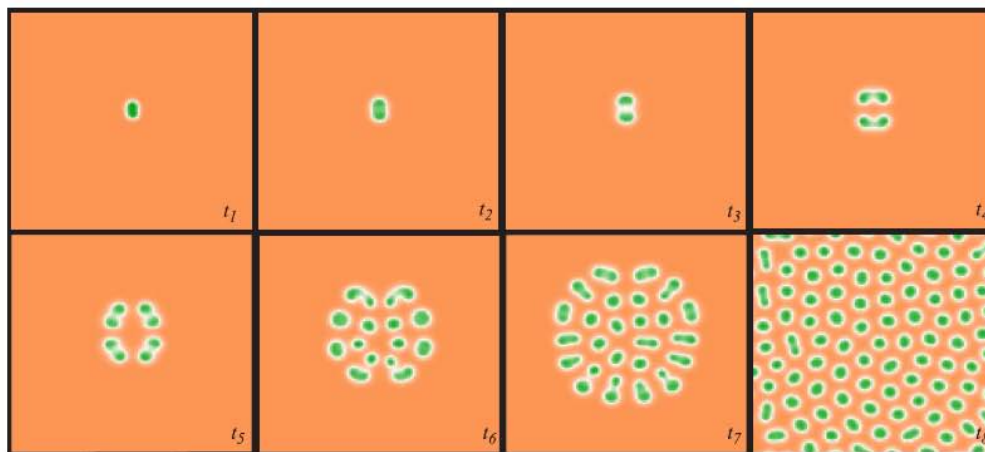The Fourier transform is used considering the binary image $U(x,y)$ of the structures detected. It is defined as

$$\widehat{U}(k_x, k_y) = \int \int_{-\infty}^{\infty} U(x,y) \exp(-2\pi i (k_x x + k_y y)) \, dx \, dy \qquad (7)$$

where (x,y) are the spatial coordinates of the image pixels, and (k_x, k_y) are the spatial frequencies, usually $\widehat{U}$ is referred to as the spectrum of U. Peaks in the spectrum indicate dominant wavelengths or typical sizes of the patches detected in the satellite images (see Couteron and Lejeune, 2001; Deblauwe et al., 2011).

3. Results

3.1. Self-replication: From vegetation patches to extended pattern

Detailed mathematical analysis is provided for the first time for Eq. (1) (see the Appendix A.1). This analysis shows that under a wide range of the aridity parameter, there is coexistence between homogeneous and pattern states. Thus, supporting stable localized vegetation patches. Moreover, as observed in models with only local interactions (Bordeu et al., 2016), vegetation patches in the non-local model may also be affected by a Turing-Prigogine instability, where the patch elongates, increasing in size to finally split into two patches, through the decay of the central "bridge" that connected them. This *mitotic* dynamics occurs repeatedly to each of the new patches, allowing the single initial patch to end up covering the whole system, through the formation of a periodic hexagonal pattern, as can be observed in Fig. 2. It is through the self-replication mechanism that a single vegetation patch can induce a increase in the total biomass of a system although the aridity is too high to allow for an homogeneous cover of vegetation. Fig. 6 shows the increase of the total biomass on the transition from a single to four patches through self replication (Fig. 3).
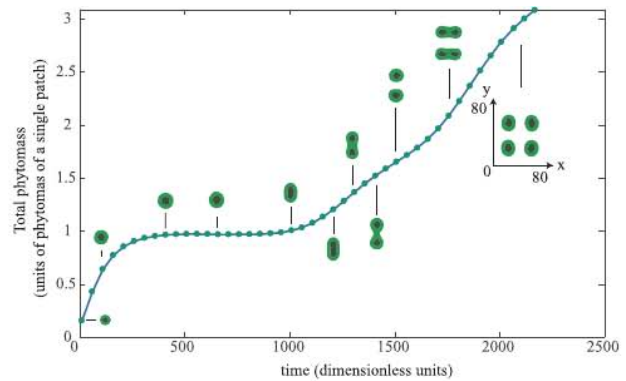
Fig. 3. Evolution of the total biomass on the transition from a single to four patches through self replication. Points obtained through direct simulation of Eq. (1), for a system of size 128×128-points, and parameters: $\mu = 1.02$, $L_c = 4.50$, $\chi_f = 2$, $\chi_c = 1$, $D = 1$, $dt = 0.1$, and $dx = 1.0$. Multiplicative noise amplitude 0.1, facilitates the initial break of symmetry. The insets show the different stages of the evolution. The total biomass is normalized with respect to the total biomass of a mature patch. Thus, during maturation a single spot reaches a normalized biomass of 1, to replicate into two patches to reach a total of almost 2. After a second replication (four patches) the system reaches a normalized biomass of 3.

To study the parameter zone where self-replication is observed, we have performed a direct numerical approach for computing the rate at which the elongating unstable mode grows, see Fig. 4. We have found that given a size-scale, L_c, for the nonlocal interactions in Eq. (1), there is a wide range of aridity, μ, for which an initial localized structure will destabilize through the self-replicating mechanism (see Fig. 4). Lower values of L_c, imply shorter-range nonlocal effects, this generates a left-shift in the self-replicating window to lower values of aridity as can be seen in Fig. 4 when comparing the red ($L_c = 4.25$, *) and yellow ($L_c = 4.00$, °) curves to the blue curve ($L_c = 4.50$, ×).

Moreover, we have found that for aridity parameter values below the self-replicating region, there is a different route for the self-replicating mechanism (see ring instability inset, Fig. 4), here, an initial localized structure grows radially. After reaching a critical radius, the central portion of the structure decays, forming a doughnut-like shape. This structure is also unstable. By the consequent decay of two opposite sides of the doughnut, the structure ends up dividing into two new localized patches.

Following the simulations of a single initial localized patch (Fig. 2), we performed large-scale simulations, containing hundreds of randomly distributed patches, the objective of this, was to assess how
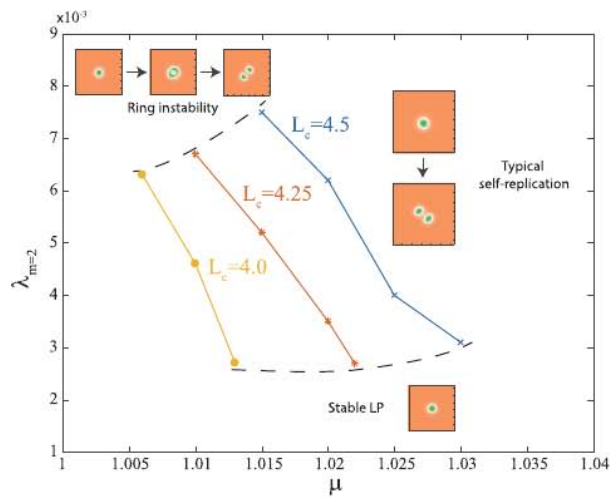

Fig. 2. Evolution of a self-replicating localized vegetation patch, for a sequence of time points $t_1 < t_2 < \ldots < t_5 < t_6$. Obtained through direct simulation of Eq. (1), for a system of size 128×128-points, and parameters: $\mu = 1.02$, $\chi_f = 2$, $\chi_c = 1$, $L_c = 4.5$, $D = 1$, $dt = 0.1$, and $dx = 1.0$.

Fig. 4. Growth rate of the unstable mode, corresponding to an elongation, leading to division. For: (×) $L_c = 4.50$; (∗) $L_c = 4.25$; (○) $L_c = 4.00$, as a function of the aridity parameter μ. Lines are linear interpolations. Outside the limits denoted by dashed lines, initial localized structures may remain stable (large μ values), or destabilize through a ring instability, leading to division (smaller μ values). Points obtained through direct simulation of Eq. (1), for a system of size 128×128-points, and parameters: $\chi_f = 2$, $\chi_c = 1$, $D = 1$, $dt = 0.1$, and $dx = 1.0$. Multiplicative noise amplitude 0.1, facilitate the initial break of symmetry.

fundamental is the self-replicating process in the emergence of the characteristic wavelength in the system. We proceeded as follows: (i) Considering a system of 256×256-points ($dx = 2.0$), we built and initial condition consisting of a spatial Poisson point process with rate 0.001, this generates on the order of 600 points randomly distributed in the two-dimensional plane. Each of the points is considered as the center of a localized patch of 3-points radius, the generated state can be observed in Fig. 5a. (ii) The random field is used as initial condition for simulating Eq. (1) for a parameter region inside the self-replication windows (see Fig. 4, $L_c = 4.50$). (iii) We let the system evolve, and obtain a transient state, that can be seen in Fig. 4c, although here we cannot observe new structures, because the evolution time was too short, it is enough time for the system to split the existing cluster into distinct structures.

When computing the Fourier transform of both the initial and the evolved state, we see that for the case of the initial state (Fig. 5b) the Fourier transform (apart from the central peak) exhibits a characteristic wavelength of the order of the size of the localized structures ($\lambda = 3$ A.U), due to the almost mono-dispersed sizes of the computer generated structures (almost, because some of the structures merged to generate bigger clusters), the same phenomenon was observable in the analysis of Zambia's landscape (Fig. 5c).

On the contrary, when analyzing the evolved state (Fig. 5d), we see immediately the emergence of a characteristic wavelength much larger than the size of the structures ($\lambda = 14$ A.U.), this wavelength emerges as a result of the self-organizing nature of the system, where clusters split, rapidly arriving at a characteristic distribution.
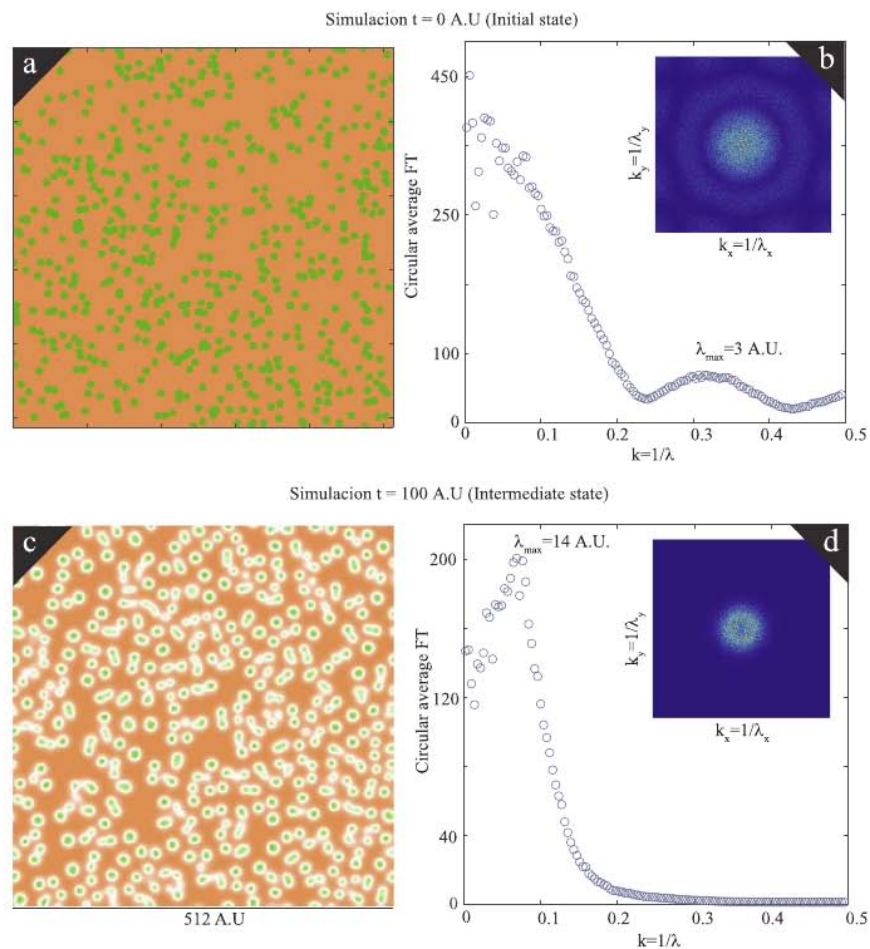

Fig. 5. Large scale simulations, (a, b)-shows the 256×256-point ($dx = 2.0$) initial condition generated from a Poisson point process with structures of 3-point radius, and its corresponding Fourier transform, respectively. (c, d)-Shows the evolved state after 1000 iterations ($dt = 0.1$), and the corresponding Fourier transform, respectively. Parameter: $\mu = 1.02$, $L_c = 4.5$, $\chi_f = 2$, $\chi_c = 1$, and $D = 1$. Measurements done in dimensionless units (A.U.).
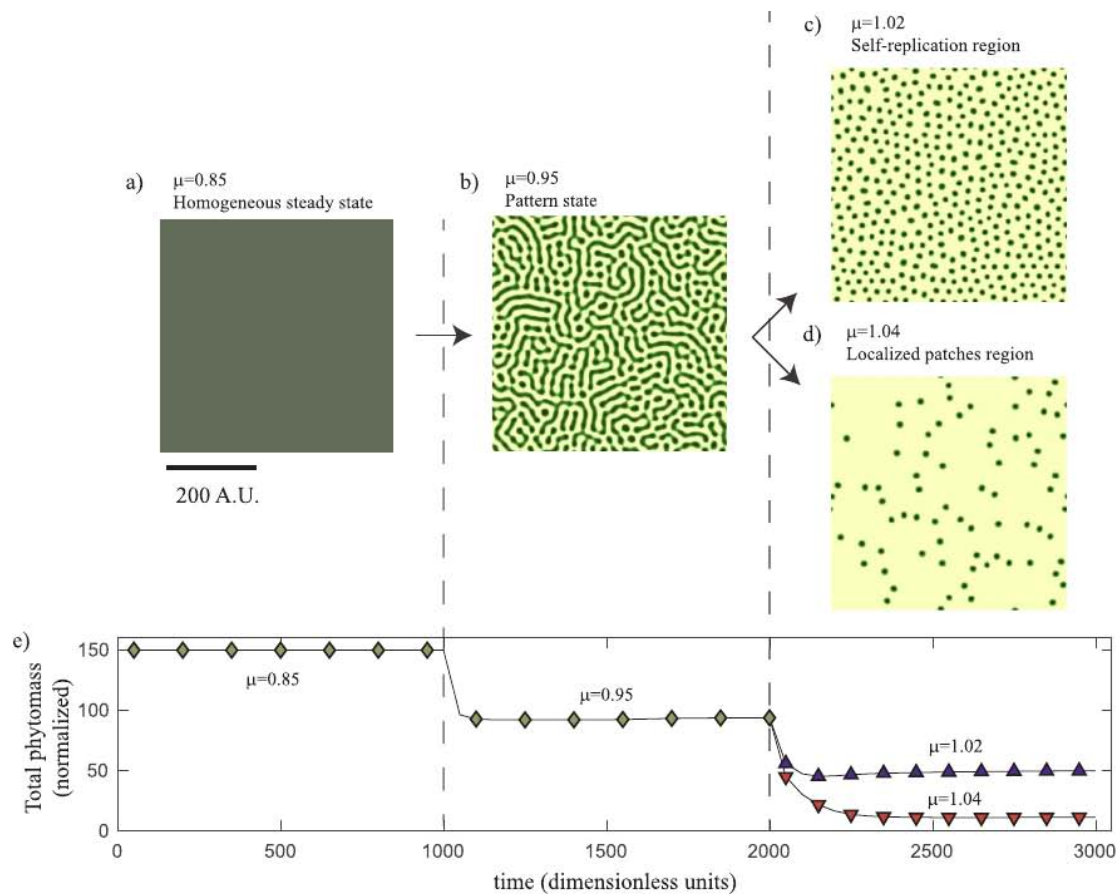
Fig. 6. Fragmentation: homogeneous cover decays as aridity increases. (a) $\mu = 0.85$, initial condition, the system is in a completely vegetated state. (b) $mu = 0.95$ the homogeneous state decays to a labyrinthine pattern. (c) $mu = 1.02$, (self replicating region) labyrinthine pattern decays to a non-periodic patch pattern. (d) $mu = 1.04$, (stable localized patches region) labyrinthine pattern decays to isolated patches without evident global order. (e) Shows the temporal evolution of the total biomass (normalized by the biomass of a the single LP in Fig. 3), diamonds show the transition from $\mu = 0.85$ to $\mu = 0.95$, upward-triangles show the transition to $\mu = 1.04$, while downward-triangles show the transition to $\mu = 1.02$. Simulation parameters: 256×256-point grid ($dx = 2.0$), $dt = 0.1$, $L_c = 4.5$, $\chi_f = 2$, $\chi_c = 1$, and $D = 1$. Multiplicative noise with amplitude 0.01 is used to facilitate the initial destabilization of the homogeneous state.

3.2. Fragmentation: from homogeneous cover to patchy landscapes

We have shown that through self-replication a single or multiple localized patches may increase the total biomass of a system leading ultimately to a hexagonal patterned state. However this is not the only route by which a system can reach such patterned state, a second route is presented in Fig. 6, where an homogeneous vegetated state ($\mu = 0.85$) is destabilized by an increase in aridity towards a labyrinthine pattern ($\mu = 0.95$). Further increasing aridity drives the system towards two possible final states, the first possibility is a reduction in aridity that takes the system to the region where localized patches are unstable and suffer from self-replication ($\mu = 1.02$), here, the labyrinthine pattern breaks down into multiple localized patches that cover the system by generating a patterned state. Note that the bare state become stable when $\mu > 1$. On the other hand, when aridity is shifted from $\mu = 0.95$ to $\mu = 1.04$, where localized patches are stable, then the system reaches a different state, consisting on a low number of isolated patches distributed in a disordered manner.

It is important to mention that a discontinuous transition from the stable homogeneous cover region ($\mu = 0.85$) directly to any of the non-periodic patch regions ($\mu = 1.02$ or 1.04) generates an overall decay of the homogeneous state to the bare state. Thus, an intermediate level of aridity is necessary for allowing the destabilization of the homogeneous cover into a non-periodic patch pattern.

3.3. Remote-sensing observations

We have studied the spatial distribution of localized patches in eight distinct regions, four located in the Fombeni region, Mozambique, and other four located in the Mufumbwe District, North-Western Province of Zambia. The vegetation in Zambia is dominated be a medium size tree *Brachystegia spiciformis*. The vegetation patterns observed in these regions are not periodic, and are composed by vegetation patches, possibly composed by groups of trees forming compact clusters. Each patch can cover an area of up to thousands square-meters, with an effective radius of tens of meters, as can be observed in Fig. 1a and f (and SI Figs. 11 and 12).

The maximal values of the radius of the structures extends over hundreds of meters, however, the typical value (mode) varies from region to region, ranging from 7 meters (zones 3, and zone 4 in Zambia) up to 36 meters (Zambia zone 4), most of the regions show a marked characteristic size of the structures (see Fig. 7a and f, and SI Figs. 11 and 12) and nearest-neighbor distance (see Fig. 7b and g), indicating a preferred spatial patch distribution.

To study the spatial organization of the patterns, we perform two measurements, the first is a modified Ripley's function L, which measures the level of clustering of a spatial point process (see formula (5)), and the second one is the radial distribution function (6), used to measure the correlation in a point process. Both observables are closely related (Couteron and Kokou, 1997), yet together they allow for further
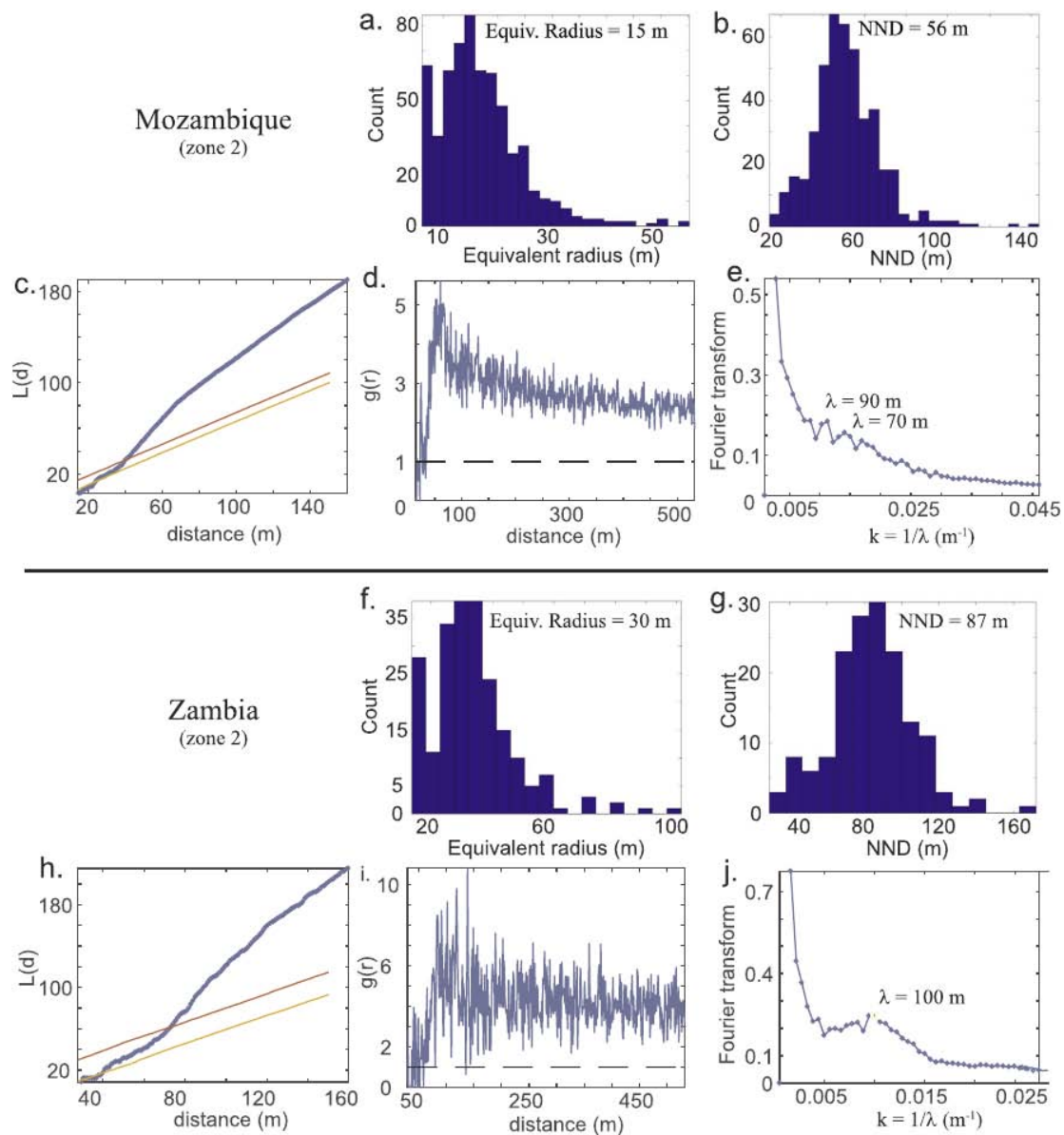
Fig. 7. Measurements performed on the detected patches for *zones 2* of Mozambique (top) and Zambia (bottom). (a) & (f) show the histograms for the equivalent radii of the structures and (b) and (g) show the histogram of the nearest-neighbor distances between them. the modified K-function $L(r)$ (lines show the 95% confidence interval) shown in (c) and (h), while (d) and (i) show the radial distribution function $g(r)$. Finally the circular average of the two-dimensional Fourier transform, i.e, the spectra are shown in (e) and (j).

insight into the spatial organization. All regions Zambia and zones 1 and 4 in Mozambique exhibit scarcity of neighbors at close distance (observations below the 95% confidence interval) and then transition towards clustering is observed for larger distances (Fig. 7c and h). Similarly, when analyzing the correlation of the point distribution through the radial distribution function, we observe a positive correlation ($g(r) > 1$) regime in all the zone, in particular, regions with high clustering exhibit long range positive correlation, while zones 1 and 3 in Mozambique, which show no clustering exhibit a positive correlation only for a small distance (Fig. 7d and i). Because of the size of the regions considered (see SI Fig. 10) where the terrain is not homogeneous, and there is a qualitative change in the structures even within a single zone, this prevents the definition of a characteristic wavelength through a spatial Fourier transform on every region. Positive examples are zones 2 in Mozambique and Zambia, where an incipient characteristic wavelength can be defined (Fig. 7e and j).

To study if there is a relationship between the size of the patches and the distance between them, we make use of the results from the analysis of radius and nearest-neighbor distance (NND) between structures (see SI Figs. 11 and 12) and study the correlation between them through a linear correlation analysis (see Fig. 8). We observe a strong correlation between the two quantities, indicating that there might be a underlying mechanism controlling both the structures size and the distance between them.

4. Discussion

Numerical observations of the non-local model studied suggest that self-replication may be an important path for the propagation of vegetation, which allows for the propagation of the vegetation even in arid conditions where the homogeneous cover is not viable due to the lack of resource (nutrients and/or water). Moreover, it has been shown
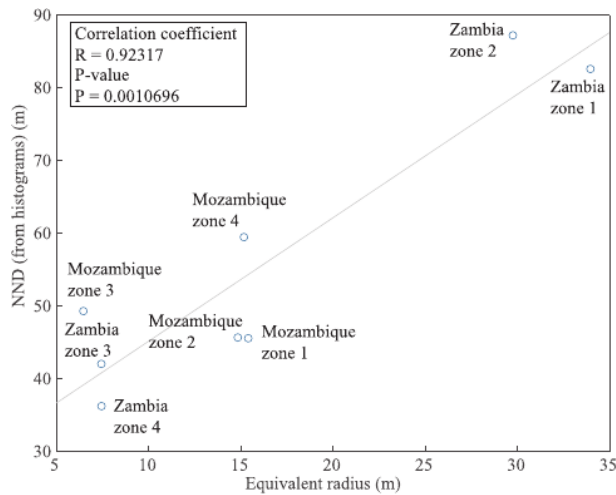
Fig. 8. Correlation between the mean equivalent radius of the structures and the nearest-neighbor distance for each of the eight regions analyzed, there is a positive linear correlation between these two quantities ($P < 0.05$), which allow us to discard the null hypotheses.

that a transition from a homogeneous vegetation cover to a patch patterned state may only occur if the transition occurs towards the self-replicating region. However, in real-ecosystems processes occur at a slow time scale and there is a high number of uncontrolled parameters which prevent the assessment of the validity of the numerical observations. We however illustrate the plausibility of the process by referring to observations at a single point in time of patchy vegetation in Africa.

The properties of the landscapes observed in Mozambique and Zambia show some indications that support self-organization. These systems exhibit a characteristic distance between patches, and a characteristic patch size, together with clustering and long range correlations in the spatial distribution. This may indicate that patches are interacting with each other resulting in the spatial distributions observed. From our modeling perspective, localized patches which are too close to each other (high density) will compete for resources ending up with the disappearance of the one placed in the less favourable location. If the patches are too far apart (low density), the extra space will allow the growth of the patches resulting in self-replication and the formation of new patches that will fill the previously unoccupied region. We must here make clear that we cannot corroborate the existence of these dynamical processes from the data analysis performed. The remote sensing data provides no temporal information and limited spacial resolution. Further on-site investigations are necessary to comprehend plant-plant interaction in specific contexts, and to assess if there are local factors that contribute to the self-organization of the landscape.

Despite all of this, we have observed features that support the patch self-replication hypothesis, for example, the observation of rings, which is a second route to self-replication (see Fig. 4). Rings are usually transient state, leading to division into two or more patches (Bordeu et al., 2016; Meron et al., 2004). Examples of this can be observed in different regions of Zambia (for example, [14°40′10.36″S, 25°49′37.34″E], and the surrounding areas). It is harder to observe the formation of rings in Mozambique, and we believe this relates to the facts that the structures in this location are smaller, preventing the ring instability to take place. Moreover the direct correlation between the size of the patches and the nearest neighbor distance, is also rendered by the model, which indicates that there is a dominant wavelength in the system that controls both the size of the structures and distance between them. This wavelength depends on the aridity parameter (see Appendix A.1).

5. Conclusions and perspectives

By making use of a generic interaction redistribution model, and by

establishing new theoretical results in the most general case (instead of an approximation of the model as in Bordeu et al. (2016)), we have shown that self replication of localized patches is generically present even in the most general model involving non-local competition and facilitating interactions. We have shown, through this model, that a localized structure may undergo multiple self-replications to finally cover the whole space available with a regular hexagonal pattern, and by doing so, let the total biomass in the system increase in time. Moreover, the self-replication regime may be an important stage in the decay of homogeneous covers of vegetation to hexagonal pattern states. It may be seen as an alternative to a more abrupt decay in biomass without this, the decay in the biomass is more abrupt resulting in a low number of sparse patches. We hypothesize that these processes are occurring in the observed landscapes of Mozambique and Zambia. The model has allowed us to provide theoretical predictions of the space-time evolution of the biomass as a function of the level of the aridity. This could be used as an indicator to identify whether stressed ecological systems may self-replicate or, on the contrary exhibit decaying dynamics.

Through the analysis of satellite images, we have given evidence to support the self-organization hypothesis. Despite the limited amount of data, which prevents being assertive about the underlying processes, we believe that self-replication could be considered as a possible mechanism for the regeneration dynamics of these landscapes. This phenomenon may occur for a moderate level of the aridity. Moreover, when considering a homogeneous cover, a gradual increasing of the level of the aridity results in a decay of the total biomass. The degradation of the ecosystems though fragmentation leads to either a periodic vegetation patterns or a random distribution of localized patches of vegetation. However, a periodic pattern is only obtained if the system relaxes in the region where self-replication exists, and patches are unstable.

As mentioned in the Discussion section, more data, specially field measurements, long time-lapse imaging and controlled experiments are necessary to confirm any claim on the nature of the observed patterns. However, measurements done here are a first step to understand the distribution of the observed patterns, and illustrate that self-organization is a strong candidate to explain them. Despite that there is no direct observations of self-replication, the current state of some patches drive us to think that self-replication might be an ongoing process, for example in the "dividing" patches showed in Fig. 1.

The knowledge of the below-ground structures of the type of vegetation considered in this contribution is rather limited. From the current literature only rooting depth data and a quantitative index of the vertical distribution of roots are available, which are irrelevant for the present study. Moreover, the full lateral roots extension has not yet been measured. For this reasons it was beyond the scope of the present contribution to perform a quantitative comparison between theoretical results and field observations. On the other hand, the model presented here has been previously confronted quantitatively to experimental measurement for two type of plants (Festuka orthophylla Couteron et al., 2014 and Combretum micranthum Barbier et al., 2006; Barbier et al., 2008; Lefever et al., 2009). We believe that the same measurement could be realized for the type of vegetation of Zambia and Mozambique.

Appendix A

A.1. Stability analysis of the integro-differential model

The stationary homogeneous states of Eq. (1), describing uniform vegetation covers, are $b_0 = 0$, and b_s, given by the solutions of

$$\mu = (1-b_s)\exp(\Lambda b_s),\tag{8}$$

where the feedback difference $\Lambda \equiv \chi_f - \chi_c$ measures the community cooperativity. The first, $b_0 = 0$, represents a territory totally devoid of vegetation, i.e., a bare state. The second, b_s corresponds to uniform plant distributions that can be either monostable if $\Lambda < 1$ or bistable when $\Lambda > 1$. In the monostable case, $\Lambda < 1$, the biomass density decreases monotonously with the aridity parameter μ and vanishes at $\mu = 1$ (cf. Fig. 9). It exist only if $\mu < 1$. In the bistable case, $\Lambda > 1$, the uniform plant distributions extends up to the turning point sometimes also referred to as tipping point (saddle-node bifurcation point). The coordinates of this point are $b_l = (\Lambda-1)/\Lambda$ and $\mu_l = \exp(\Lambda-1)/\Lambda$.

To study the linear stability analysis of the stationary homogeneous states, b_s, we introduce a small amplitude deviations from b_s of the form

$$b(\mathbf{r},t) = b_s + \varepsilon\exp(\lambda(k)t + i\mathbf{k}\cdot\mathbf{r}),\tag{9}$$

where ε is a small parameter and the deviation from the b_s is expressed in terms of Fourier modes $\exp(\lambda(k)t + i\mathbf{k}\cdot\mathbf{r})$ in the space of wavevector $\mathbf{k}$. By replacing Eq. (9) and by linearizing with respect to ε, the dispersion relation obeyed by the eigenvalues $\lambda(k)$ reads

$$\lambda(k) = \left[\chi_f(1-b_s)-1-\frac{\chi_c(1-b_s)}{(1 + (kL_c)^2)^{3/2}}\right]b_s e^{\chi_f b_s} - Dk^2.\tag{10}$$

The critical points associated with the Turing-Prigogine instability are given by,

$$\left.\frac{\partial\lambda}{\partial k}\right|_{b_s=b_c,k=k_c} = 0,\tag{11}$$

$$\lambda(k_c) = 0.\tag{12}$$

These two conditions provide the thresholds $b_c = b_{TP}$ and the most unstable wavenumber $k_c = k_{TP}$ associated with the Turing-Prigogine instability. The critical wavenumber at the onset of the instability is given explicitly by

$$k_{TP}^2 = \frac{1}{L_c^2}\left[\left(\frac{\chi_c b_{TP}(1-b_{TP})e^{\chi_f b_{TP}}L_c^2}{2D}\right)^{\frac{2}{5}}-1\right].\tag{13}$$

The wavelength is $2\pi/k_{TP}$. The above equation has two solutions, which we denote by (k_{TP1},b_{TP1}) and (k_{TP2},b_{TP2}). The thresholds associated with the Turing-Prigogine instability are solutions of

$$[\chi_f(1-b_{TP})-1]e^{\chi_f b_{TP}} = 3\left(\frac{D}{L_c^2}\right)^{\frac{3}{5}}\left[\frac{\chi_c b_{TP}(1-b_{TP})e^{\chi_f b_{TP}}}{2}\right]^{\frac{2}{5}}-\left(\frac{D}{L_c^2}\right).\tag{14}$$

The results of the linear stability analysis are summarized in Fig. 9. As the aridity level μ increases, the vegetation evolves toward extinction. For $0 < \Lambda \leqslant 1$, the decrease of the phytomass density is monotonous. The bare state density is reached at the switching point $\mu = 1$, where the plant distribution state is destabilized through the Turing-Prigogine instability (Turing, 1952; Prigogine and Lefever, 1968). In the range $b_{TP1} < b < b_{TP2}$, the uniform phytomass state is unstable. The corresponding levels of the aridity μ_{TP} are obtained from the homogeneous steady states Eq. (8) (see Fig. 9).
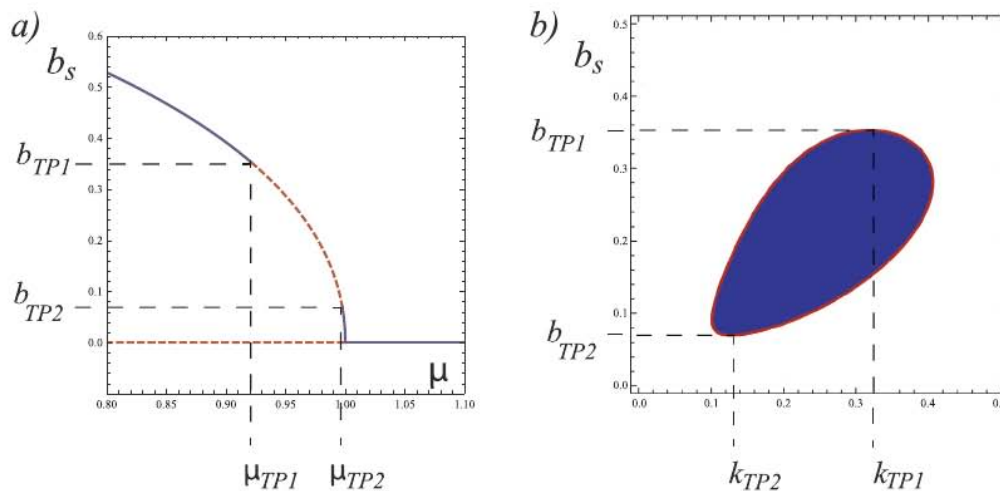

Fig. 9. Stability diagrams. (a) Uniform stationary distributions of the biomass density b_s, and their stability with respect to homogeneous and inhomogeneous perturbations are plotted as a function of the aridity parameter μ. Stable states are indicated by solid line, and unstable ones are represented by dotted lines. (b) The marginal stability curve in the $(b_s$-$k)$ plane. The domain of instability for is represented by a blue shaded area delimited by red solid line. Parameter are $\chi_f = 2$, $\chi_c = 1$, $L_c = 4$, and $D = 1$.

When increasing the stress or aridity, the wavelength of the corresponding pattern increases, and simultaneously the morphology of the vegetation pattern changes, this is related to the observations made in Mozambique and Zambia, where an increase in the system wavelength is directly correlated with an increase in the size of the vegetation patches. The generic sequence of spatially periodic states obtained for increasing aridity is: spots of lower density forming an hexagonal lattice, alternating stripes of higher and lower density, and spots of higher density forming an hexagonal lattice (Lejeune and Tlidi, 1999; Lejeune et al., 2004). This behavior has been also found for other mathematical models that include water transport by underground diffusion and/or above ground run-off (von Hardenberg et al., 2001; Rietkerk and Van de Koppel, 2008; Sherratt, 2013; Gowda et al., 2014).

Appendix B. Supplementary data

Supplementary data associated with this article can be found, in the online version, at http://dx.doi.org/10.1016/j.ecolind.2018.02.009.

References

Barbier, N., Couteron, P., Lejoly, J., Deblauwe, V., Lejeune, O., 2006. Self-organized vegetation patterning as a fingerprint of climate and human impact on semi-arid ecosystems. J. Ecol. 94 (3), 537–547.

Barbier, N., Couteron, P., Lefever, R., Deblauwe, V., Lejeune, O., 2008. Spatial decoupling of facilitation and competition at the origin of gapped vegetation patterns. Ecology 89 (6), 1521–1531.

Bordeu, I., 2016. Labyrinthine dissipative patterns. J. Phys.: Conf. Ser. 720 (1), 012004.

Bordeu, I., Clerc, M.G., Couteron, P., Lefever, R., Tlidi, M., 2016. Self-replication of localized vegetation patches in scarce environments. Sci. Rep. 6, 33703.

Brooker, R.W., Maestre, F.T., Callaway, R.M., Lortie, C.L., Cavieres, L.A., Kunstler, G., Liancourt, P., Tielbörger, K., Travis, J.M., Anthelme, F., Armas, C., Coll, L., Corcket, E., Delzon, S., Forey, E., Kikvidze, Z., Olofsson, J., Pugnaire, F., Quiroz, C.L., Saccone, P., Schiffers, K., Seifan, M., Touzard, B., Michalet, R., 2008. Facilitation in plant communities: the past, the present, and the future. J. Ecol. 96 (1), 18–34.

Champneys, A.R., 1998. Homoclinic orbits in reversible systems and their applications in mechanics, fluids and optics. Physica D 112 (1–2), 158–186.

Coullet, P., Riera, C., Tresser, C., 2000. Stable static localized structures in one dimension. Phys. Rev. Lett. 84 (14), 3069.

Couteron, P., Kokou, K., 1997. Woody vegetation spatial patterns in a semi-arid savanna of Burkina Faso, West Africa. Plant Ecol. 132 (2), 211–227.

Couteron, P., Lejeune, O., 2001. Periodic spotted patterns in semi-arid vegetation explained by a propagation-inhibition model. J. Ecol. 89 (4), 616–628.

Couteron, P., Anthelme, F., Clerc, M., Escaff, D., Fernandez-Oto, C., Tlidi, M., 2014. Plant clonal morphologies and spatial patterns as self-organized responses to resource-limited environments. Philos. Trans. R. Soc. A 372 (2027), 20140102.

Dakos, V., Kéfi, S., Rietkerk, M., Van Nes, E.H., Scheffer, M., 2011. Slowing down in spatially patterned ecosystems at the brink of collapse. Am. Nat. 177 (6), E153–E166.

Deblauwe, V., Couteron, P., Lejeune, O., Bogaert, J., Barbier, N., 2011. Environmental modulation of self-organized periodic vegetation patterns in sudan. Ecography 34 (6), 990–1001.

Deblauwe, V., Couteron, P., Bogaert, J., Barbier, N., 2012. Determinants and dynamics of banded vegetation pattern migration in arid climates. Ecol. Monogr. 82 (1), 3–21.

Gowda, K., Riecke, H., Silber, M., 2014. Transitions between patterned states in vegetation models for semiarid ecosystems. Phys. Rev. E 89 (2), 022701.

HilleRisLambers, R., Rietkerk, M., van den Bosch, F., Prins, H.H., de Kroon, H., 2001. Vegetation pattern formation in semi-arid grazing systems. Ecology 82 (1), 50–61.

Kaminaga, A., Vanag, V.K., Epstein, I.R., 2005. black spots in a surfactant-rich belousov–zhabotinsky reaction dispersed in a water-in-oil microemulsion system. J. Chem. Phys. 122 (17), 174706.

Kéfi, S., Rietkerk, M., Alados, C.L., Pueyo, Y., Papanastasis, V.P., ElAich, A., De Ruiter, P.C., 2007. Spatial vegetation patterns and imminent desertification in mediterranean arid ecosystems. Nature 449 (7159), 213.

Kéfi, S., Rietkerk, M., van Baalen, M., Loreau, M., 2007. Local facilitation, bistability and transitions in arid ecosystems. Theor. Popul. Biol. 71 (3), 367–379.

Klausmeier, C.A., 1999. Regular and irregular patterns in semiarid vegetation. Science 284 (5421), 1826–1828.

Knobloch, E., 2015. Spatial localization in dissipative systems. Ann. Rev. Condens. Matter Phys. 6 (1), 325–359.

Kolokolnikov, T., Tlidi, M., 2007. Spot deformation and replication in the two-dimensional belousov-zhabotinski reaction in a water-in-oil microemulsion. Phys. Rev. Lett. 98 (18), 188303.

Lee, K.J., McCormick, W.D., Pearson, J.E., Swinney, H.L., 1994. Experimental observation of self-replicating spots in a reaction–diffusion system. Nature 369 (6477), 215.

Lefever, R., Lejeune, O., 1997. On the origin of tiger bush. Bull. Math. Biol. 59 (2), 263–294.

Lefever, R., Turner, J.W., 2012. A quantitative theory of vegetation patterns based on plant structure and the non-local f-kpp equation. Comptes Rendus Mécanique 340 (11–12), 818–828.

Lefever, R., Barbier, N., Couteron, P., Lejeune, O., 2009. Deeply gapped vegetation patterns: on crown/root allometry, criticality and desertification. J. Theor. Biol. 261 (2), 194–209.

Lejeune, O., Tlidi, M., 1999. A model for the explanation of vegetation stripes (tiger bush). J. Vegetation Sci. 10 (2), 201–208.

Lejeune, O., Tlidi, M., Couteron, P., 2002. Localized vegetation patches: a self-organized response to resource scarcity. Phys. Rev. E 66 (1), 010901.

Lejeune, O., Tlidi, M., Lefever, R., 2004. Vegetation spots and stripes: dissipative structures in arid landscapes. Int. J. Quantum Chem. 98 (2), 261–271.

Mawhin, J., 2002. Les héritiers de pierre-françois verhulst: une population dynamique. Acad. R. Belg. Bull. Cl. Sci.(6) 13, 349–378.

Meron, E., 2015. Nonlinear Physics of Ecosystems. CRC Press, Taylor & Francis Group.

Meron, E., Gilad, E., von Hardenberg, J., Shachak, M., Zarmi, Y., 2004. Vegetation patterns along a rainfall gradient. Chaos Solitons Fractals 19 (2), 367–376.

Pearson, J.E., 1993. Complex patterns in a simple system. Science 261 (5118), 189–192.

Pomeau, Y., 1986. Front motion, metastability and subcritical bifurcations in hydrodynamics. Physica D 23 (1–3), 3–11.

Prigogine, I., Lefever, R., 1968. Symmetry breaking instabilities in dissipative systems. ii. J. Chem. Phys. 48 (4), 1695–1700.

Rietkerk, M., Van de Koppel, J., 2008. Regular pattern formation in real ecosystems. Trends Ecol. Evol. 23 (3), 169–175.

Rietkerk, M., Dekker, S.C., De Ruiter, P.C., van de Koppel, J., 2004. Self-organized patchiness and catastrophic shifts in ecosystems. Science 305 (5692), 1926–1929.

Ripley, B.D., 1976. The second-order analysis of stationary point processes. J. Appl. Prob. 13 (2), 255–266.

Schenk, H.J., Jackson, R.B., 2002. Rooting depths, lateral root spreads and below-ground/above-ground allometries of plants in water-limited ecosystems. J. Ecol. 90 (3), 480–494.

Sherratt, J.A., 2013. History-dependent patterns of whole ecosystems. Ecol. Complexity 14, 8–20.

Tlidi, M., Mandel, P., Lefever, R., 1994. Localized structures and localized patterns in optical bistability. Phys. Rev. Lett. 73 (5), 640.

Tlidi, M., Vladimirov, A.G., Mandel, P., 2002. Curvature instability in passive diffractive resonators. Phys. Rev. Lett. 89 (23), 233901.

Tlidi, M., Lefever, R., Vladimirov, A., 2008. On vegetation clustering, localized bare soil spots and fairy circles. In: Dissipative Solitons: From Optics to Biology and Medicine. Springer, pp. 1–22.

Tlidi, M., Staliunas, K., Panajotov, K., Vladimirov, A.G., Clerc, M.G., 2014. Localized structures in dissipative media: from optics to plant ecology. Philos. Trans. R. Soc. A 372, 20140101.

Turing, A.M., 1952. The chemical basis of morphogenesis. Philos. Trans. R. Soc. London Ser. B 237 (641), 37–72.

Verhulst, P.F., 2013. Recherches mathématiques sur la loi d'accroissement de la population. Nouveaux Mémoires de l'Académie Royale des Sciences et Belles-Lettres de Bruxelles 18, 1–42.

Vesipa, R., Camporeale, C., Ridolfi, L., 2015. Noise-driven cooperative dynamics between vegetation and topography in riparian zones. Geophys. Res. Lett. 42 (19), 8021–8030.

Vladimirov, A.G., Lefever, R., Tlidi, M., 2011. Relative stability of multipeak localized patterns of cavity solitons. Phys. Rev. A 84 (4), 043848.

von Hardenberg, J., Meron, E., Shachak, M., Zarmi, Y., 2001. Diversity of vegetation patterns and desertification. Phys. Rev. Lett. 87 (19), 198101.